*Biochimica et Biophysica Acta*, 1018 (1990) 29–40
Elsevier



BBABIO 43229

# Inhibitor effects on redox-linked protonations of the *b* haems of the mitochondrial $bc_1$ complex

Peter R. Rich, Alan E. Jeal, Sally A. Madgwick and A. John Moody

*Glynn Research Institute, Bodmin (U.K.)*

(Received 18 December 1989)

Key words: Cytochrome $bc_1$ complex; Cytochrome *b*; $E_m$/pH relation; Ubiquinone; Q site inhibitor

**The effects of pH and inhibitors on the spectra and redox properties of the haems *b* of the $bc_1$ complex of beef heart submitochondrial particles were investigated. The major findings were: (1) both haems have a weakly redox-linked protonatable group with $pK_{ox}$ and $pK_{red}$ of around 6 and 8; (2) at pH values above 7, haem $b_H$ becomes heterogeneous in its redox behaviour. This heterogeneity is removed by the $Q_i$ site inhibitors antimycin A, funiculosin and HQNO, but not by the $Q_o$ site inhibitors myxothiazol or stigmatellin; (3) of all inhibitors tested only funiculosin had a large effect on the $E_m$/pH profile of either haem *b*. In all cases where definite effects were found, the haem most affected was that thought to be closest to the site of inhibitor binding; (4) spectral shifts of haem groups caused by inhibitor binding were usually, but not always, of the haem group closest to the binding site; (5) titrations with succinate/fumarate were in reasonable agreement with redox-mediated data provided that strict anaerobiosis was maintained. Apparent large shifts of haem midpoint potentials with antimycin A and myxothiazol could be produced in aerobic succinate/fumarate titrations in the presence of cyanide, as already reported in the literature, but these were artefactual; (6) the heterogeneous haem $b_H$ titration behaviour can be simulated with a model similar to that proposed by Salerno et al. (J. Biol. Chem. (1989) 264, 15398–15403) in which there is redox interaction between haem $b_H$ and ubiquinone species bound at the $Q_i$ site. Simulations closely fit both the haem $b_H$ data and known semiquinone data only if it is assumed that semiquinone bound to oxidised haem $b_H$ is EPR-silent.**

## Introduction

The Q-cycle [1] has proved to be a useful model of the protonmotive action of the $bc_1$ complex and has been generally borne out by a large variety of data in mitochondrial, bacterial and chloroplast systems. The central feature of energy conservation is an electrogenic electron transfer across the membrane from a site of quinol oxidation, the $Q_o$ site, to one of quinone rereduction, the $Q_i$ site. Associated protonation/deprotonation reactions result in a net protonmotive action. There is reasonable consensus that the electrogenic charge separation is caused by two partial reactions; roughly half is associated with electron transfer between the two haems *b* and the remainder is associated with haem $b_H$ reoxidation by quinone at the $Q_i$ site [2–5]. Although there is significant evidence that the electrogenic events are the electron transfers themselves [2,4,6], the point has been raised that it might be the associated protonic changes, rather than electron transfers per se which are electrogenic [7]. Such electrogenic proton movements, which would have to occur through the protein structure along a proton well of low dielectric strength [8,9], are of particular interest from a structural point of view and might significantly alter our view of the general topology of the enzyme.

Interpretation of the results of experiments aimed at measuring the relative contributions of electrogenic electron transfer versus electrogenic proton transfer re-

Abbreviations: HQNO, 2-*n*-heptyl-4-hydroxyquinoline-*N*-oxide; NQNO, 2-*n*-nonyl-4-hydroxyquinoline-*N*-oxide; PMS, 5-methylphenazinium methosulphate (phenazine methosulphate); $Q_o$ site, the quinol oxidation and proton *O*utput site of the cytochrome $bc_1$ complex which is in contact with the cytoplasmic aqueous phase (also termed the $Q_z$ or $Q_p$ site in bacterial and chloroplast systems); $Q_i$ site, the quinone reduction and proton *I*nput site of the cytochrome $bc_1$ complex which is in contact with the *N*egative matrix aqueous phase (also termed the $Q_c$ or $Q_N$ site in bacterial and mitochondrial systems); haem $b_H$, the high potential haem of cytochrome *b*, often termed *b*-562 from its reduced $\alpha$-band maximum; haem $b_L$, the low potential haem of cytochrome *b*, often termed *b*-566 from its reduced $\alpha$-band maximum; SHE, standard hydrogen electrode; $E_h$, ambient potential vs. SHE; $E_{mx}$, midpoint potential at pH *x* vs. SHE.

Correspondence: P.R. Rich, Glynn Research Institute, Bodmin, Cornwall, PL30 4AU, U.K.

quires a detailed knowledge of the redox linked protonation reactions. Such data are most easily obtained by studies of the pH-dependence of midpoint potentials [10,11]. Unfortunately, although there is a wealth of published data which provide a general picture [2,5,11–20], the details of the redox-linked protonation chemistry of the haems *b* are still equivocal and the effects of inhibitors are little known. This situation is exacerbated by the possibility that amino acid residues in the neighbouring quinone binding pockets might themselves influence the electronations of the haems *b* and so produce a very complex relation between midpoint potential and pH. At pH 7, the $E_m$ values of $b_H$ and $b_L$ are known to be in the range 50 to 100 mV and 0 to −50 mV, respectively, and both exhibit a measurable pH-dependence. Although both haem groups are often quoted as having a $pK_{ox}$ of around 7, the data in support of this are weak or equivocal [13]. Some effects of inhibitors at a single pH [20] or of antimycin A at a range of pH values [2,19] have been reported. Uncertainty of behaviour is increased since in some cases a high potential component of haem $b_H$ has been noted [18,21]. The presence of two forms of haem $b_H$ has been suggested to favour a dimeric mode of operation of the enzyme [22]. In addition, it is likely that the properties of the haems *b* are affected in the isolated enzyme by the nature of the detergent used for solubilisation [23].

In the present work we re-examined the $E_m$/pH relations of the haems *b* in beef heart submitochondrial particles and determined the effects of several inhibitors on these relations and on individual optical spectra. Two preliminary reports have appeared [9,24].

## Materials and Methods

*Preparation of beef heart submitochondrial particles*

Beef heart mitochondria were prepared essentially following procedure 3 of Smith [25] and stored at −20°C at around 50 mg/ml in 250 mM sucrose, 50 mM Tris-HCl and 1 mM EDTA at pH 8. Submitochondrial particles were prepared from thawed mitochondria by incubation with 1 mM ATP for 10 min at 4°C followed by passage through a Yeda press at 2000 p.s.i. at a rate of 10 ml/min. After removal of unbroken mitochondria by centrifugation at $9000 \times g_{av}$ for 10 min, the submitochondrial particles were sedimented by centrifugation at $35\,000 \times g_{av}$ for 1 h. The pellets were resuspended to around 50 mg/ml in 50 mM Tris-HCl, 0.67 M sucrose and 1 mM histidine at pH 8, and were stored in small aliquots at 77 K.

*Redox potentiometry with redox mediators*

Conventional anaerobic redox titrations [11] were carried out under argon gas in a buffer of the potassium salts of 2 mM EDTA and 50 mM tartrate (pH 4.5–5.5), Mes (pH 5.6–6.5), phosphate (pH 6.6–7.5), Taps (pH 7.6–8.5) or glycine (pH > 8.5). Submitochondrial particles were used at around 10 mg/ml (final $bc_1$ complex concentration of around 2.5 μM) and 1 μg/ml gramicidin and 1 μg/ml valinomycin were present to ensure that they were fully uncoupled. Redox mediators were: anthraquinone 2-sulphonate; anthraquinone 2,6-disulphonate; methyl viologen, benzyl viologen, phenazine ethosulphate, phenazine methosulphate, 2-methyl-1,4-benzoquinone, 2,6-dimethyl-1,4-benzoquinone, trimethyl-1,4-benzoquinone, duroquinone, hexammineruthenium chloride, diaminodurene, 5-hydroxy-1,4-naphthoquinone, 2-hydroxy-1,4-naphthoquinone and 1,4-naphthoquinone-2-sulphonate (all at 20–100 μM) and 5 μM pyocyanine. 90 units/ml of catalase were also present. Potential was varied with additions of ferricyanide, dithionite (pH < 5) or NADH (pH > 5). 4 min were usually allowed for equilibration after each addition and data represent points taken in both oxidative and reductive directions.

For measurement of ambient redox potential, we used a 3 mm diameter glassy carbon rod (Sigradur K, Sigri), sealed into a PTFE sleeve (Goodfellows, Cambridge) with epoxy resin or with vaseline. Conventionally, a platinum spade or wire is used for this purpose. However, we were unable to obtain fully reproducible results at all potentials with any of our platinum samples, even if the platinum was chemically or electrochemically precleaned before use. The source of this irreproducibility probably arose from surface monolayer coverage of the platinum with species from the test solution [26] but was not pursued further. The glassy carbon, which gave good reproducibility and accuracy, was cleaned before use with 0.05 μm alumina polishing powder. The reference electrode was a silver chloride-coated silver wire in 3 M KCl or 3 M NaCl, connected to the test solution by a 3 M KCl salt bridge. The glassy carbon/reference system was calibrated against quinhydrone in anaerobic 50 mM potassium phosphate at pH 7 both before and after the experiment. The midpoint potential of quinhydrone in this medium was taken to be +296 mV [10] vs. SHE.

*Data collection*

At each ambient potential, spectra were recorded at approx. 1 nm intervals from 542 to 630 nm with a digital single beam scanning instrument which had been constructed in-house. Normally three spectra were recorded and averaged before storage. Ambient potential was recorded at the start and end of the scans. A programme accessed these accumulated scans to produce the appropriate plots of absorbance change versus averaged potential during data collection. In this way, there was no user subjectivity in data derivation. Nernstian curves for combinations of $n = 1$ components were overlaid on these plots to produce a best fit. In those cases where the haem $b_H$ plots had several components

(for example, see Fig. 2), curves were fitted only to the low potential part of the plot (but see Fig. 8 for detailed model fitting).

*Redox potentiometry with succinate/fumarate*

Beef heart submitochondrial particles were resuspended to 4 mg/ml ($bc_1$ approx. 1 μM) in 50 mM buffer (Mes, pH 5–7; potassium phosphate (pH 7.1 to 8.2); Tricine, (> pH 8.2)), 2 mM EDTA, 1 μg/ml valinomycin and 1 μg/ml gramicidin. In the aerobic titrations, 1 mM KCN was also present and in the anaerobic titrations an atmosphere of nitrogen was maintained above the sample. Titrations were normally performed in the oxidative direction after reduction with 1–2.5 mM succinate, although reductive titrations gave roughly comparable data. Haem *b* was monitored at 562–0.5(544 + 580) nm. 50% reduction of the succinate-reducible haem *b* was taken to be the point at which 25% of the dithionite-reducible signal was developed. In practice, haem *b* reduction only in the region of 25% to 50% of the dithionite-reducible signal was usually accessible with the succinate/fumarate couple and so the 'succinate-reducible haem *b*' is approximately equivalent to the low-potential form of haem $b_H$ (see Results). Midpoint potentials were calculated from the succinate/fumarate ratio at this point, and using p*K* values given by Clark [10] with $E_{m7}$ set to +24 mV.

*Sources and stability of inhibitors*

Sources of inhibitors were: antimycin A (type III) and HQNO, Sigma; myxothiazol, Boehringer; stigmatellin, a gift of Professor Dr. G. Höfle; funiculosin, a gift of Sandoz, Switzerland. They were made up to 1–10 mM in 96% ethanol and stored at −20°C in the dark. Spectra were checked occasionally for purity and stability but in no instance was any serious problem of lability encountered.

## Results

*Characteristics and deconvolution of redox titration curves in the presence of redox mediators and at low pH*

Fig. 1 illustrates typical results of a redox titration of beef heart submitochondrial particles at pH 4.8. The low pH results are discussed first since they represent the simplest situation as far as $b_H$ and $b_L$ are concerned. A triple wavelength plot of 562–0.5(542 + 582) nm produced a characteristic curve which approximated to two $n = 1$ components of roughly 0.7 : 0.3 contribution, together with a small sharp transition at around −100 mV which was caused by *b*-560 [27]. It was further possible to approximately deconvolute individual contributions from $b_H$ and $b_L$ with plots of 562–569 nm and 566–558.5 nm. Nernst $n = 1$ curves fitted to these latter deconvolutions gave midpoint potentials of

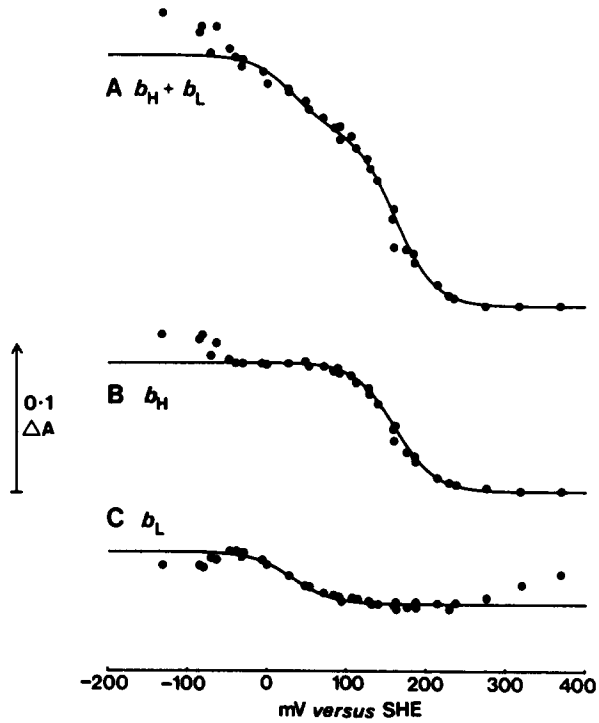


Fig. 1. Redox titration of haems *b* at pH 4.8 in beef heart submitochondrial particles. Anaerobic titrations in the presence of redox mediators were carried out at pH 4.8 as described in Materials and Methods. Data points were taken in both oxidative and reductive directions and results with several different submitochondrial particle preparations are overlaid. The plots are: (A) $b_H$ plus $b_L$ at 562–(542 + 582)/2 nm; (B) $b_H$ alone at 562–569 nm; (C) $b_L$ alone at 566–558.5 nm. At the low-potential end of the titration ($\leq -50$ mV), interference from cytochrome *b*-560 of succinate dehydrogenase can be seen on all deconvolutions. At high potentials ($\geq 250$ mV) interference from the *c*-type cytochromes can be seen on the haem $b_L$ deconvolution. These did not adversely affect midpoint potential estimation. Theoretical curves are for $n = 1$ components of $E_m$ values +161 mV (curve B) or +31 mV (curve C) or a combination of both in the ratio 0.7 : 0.3 (curve A).

+ 161 mV and +31 mV for $b_H$ and $b_L$, respectively. Curves representing these values are plotted over the data in Fig. 1. The contribution of *b*-560 to the 562–0.5(542 + 582) nm deconvolution was ignored. At higher pH values the range of potential in which *b*-560 changed its redox state did not overlap that of $b_H$ and $b_L$ and it was not considered further.

*The effects of pH on titration curves*

Fig. 2 illustrates the effects of pH on the titration curve of the haems *b*. As the pH was raised, the entire curve shifted to lower ambient potentials, as expected for electronations which have associated protonation changes, and as previously reported. In addition, the part of the curve associated with the haem $b_H$ became broader and could no longer be fitted as a single $n = 1$ redox transition. At pH 7 and above, the redox behaviour of haem $b_H$ was heterogeneous with a high potential and a low potential form separated by approx.

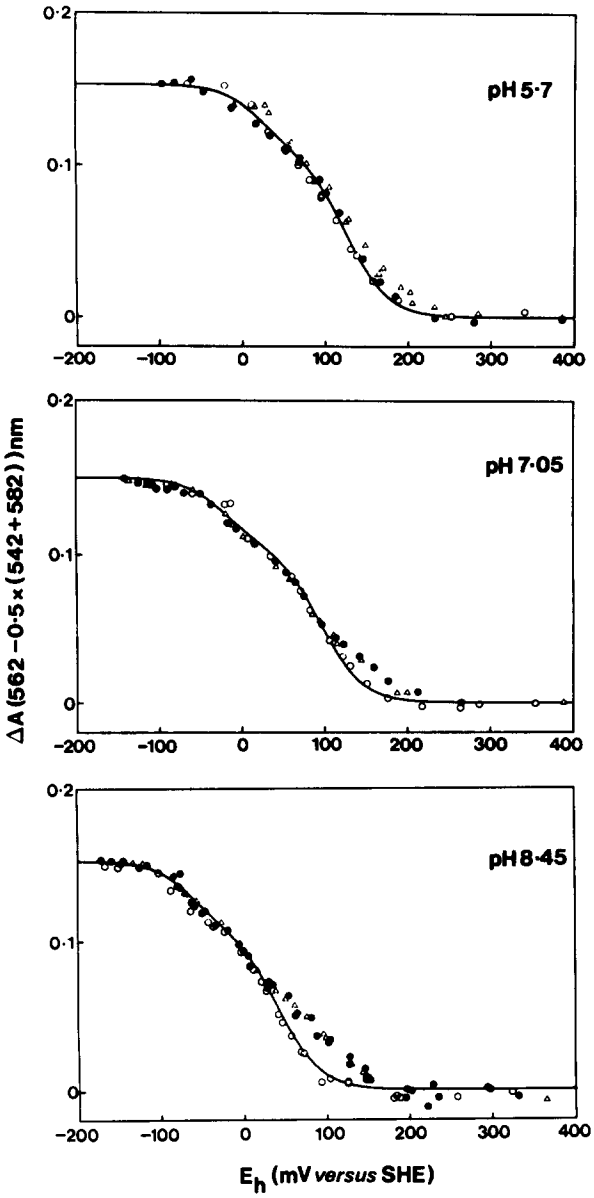


Fig. 2. The pH- and inhibitor-dependence of the redox titration curves of haems *b*. Further titrations in the presence of redox mediators were carried out in the absence of inhibitor (●) or in the presence of 5 μM antimycin A (○) or 10 μM myxothiazol (△). Data were collected within 0.1 pH units of the indicated pH, except for the myxothiazol data in the top figure, which were collected at a pH of 5.5. Only deconvolutions of $b_H$ *plus* $b_L$ at 562–(542+582) nm are shown. Theoretical curves (the values of which were derived from the deconvolutions of individual components as in Fig. 1) have been overlaid on the data which approximate best to the $b_L$ and low-potential form of $b_H$ of the control titrations. Simulations are an 0.7:0.3 ratio of two $n=1$ components of midpoint potentials: at pH 5.7, +127 and +27mV; at pH 7, +95 and −20 mV; at pH 8.4, +42 and −60 mV. All data (obtained from several different submitochondrial particle preparations) have been scaled to the same total absorbance change.

80 mV. By studying the details of spectral changes at high pH, it was found that both forms of $b_H$ had spectra which were indistinguishable from each other. No effects of pH on the individual spectra of either haem *b* could be detected.

In Fig. 2, theoretical curves are plotted over the data points. These curves represent reasonable fits of a combination of two $n=1$ components (0.3:0.7 ratio) to the $b_L$ and the low potential component only of the $b_H$ of the control data points. This illustrates clearly the marked deviation of the haem $b_H$ data which occurs as the pH is raised above pH 7. In Fig. 3, the midpoint potential values used for the fits of $n=1$ curves to the haem $b_L$ and the low-potential form of $b_H$ are plotted as a function of pH. The dependence in both cases falls short of the −58 mV/pH unit expected of components which have widely separated p$K$ values for the oxidised and reduced species. Instead, the data are mostly reasonably fitted by two components which each have a redox-linked protonatable group whose p$K$ changes from around 6 when the haem is oxidised to around 8 when the haem is reduced.

The complication and probable origin of the high potential form of haem $b_H$ which appears at high pH is evaluated in detail in the Discussion section, since the effects of inhibitors on the phenomenon, described below, are relevant to the interpretation.

*The effects of antimycin A*

Also shown in Figs. 2 and 4 are the effects of antimycin A on the redox titration curves of the haems *b* at a variety of pH values. At low pH, little or no effect of antimycin A was found on the position of the titration curves, although the characteristic red-shift of the haem $b_H$ spectrum [23] could be seen in the data at all pH values, together with a small but consistent slight shift (≈ 20 mV) downwards at low pH of the estimated midpoint potential of the $b_H$ haem. The spectrum of haem $b_L$ was unchanged. Individual components could be deconvoluted at 562–569 nm (haem $b_H$) and 566–560

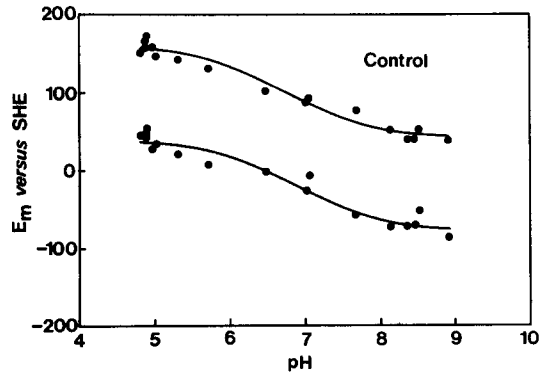


Fig. 3. $E_m$/pH plots of the *b* haems from redox-mediated titration data. The midpoint potential values of the fits to haem $b_L$ and the low-potential form of haem $b_H$ in the control data, as in Figs. 1 and 2, were plotted as a function of pH. The curves are the linear regression best fits for two components, each of which is independently redox-linked to a single protonatable group. Fitting gave for haem $b_H$, $E_o$, 160 mV, p$K_{ox}$, 5.7, p$K_{red}$, 7.7; and for haem $b_L$, $E_o$, 39 mV, p$K_{ox}$, 5.9, p$K_{red}$, 7.9.

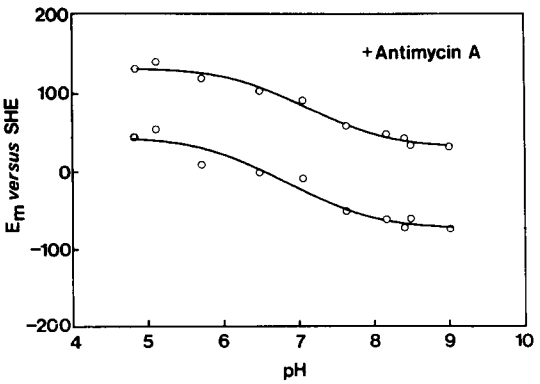


Fig. 4. $E_m$/pH plots of the *b* haems in the presence of antimycin A. The midpoint potential values of the fits to haem $b_L$ and haem $b_H$ in the presence of antimycin A were plotted as a function of pH. The curves are the linear regression best fits for two components, each of which is independently redox-linked to a single protonatable group. Fitting gave for haem $b_H$, $E_o$, 131 mV, p$K_{ox}$, 6.3, p$K_{red}$, 8; and for haem $b_L$, $E_o$, 43 mV, p$K_{ox}$, 5.8, p$K_{red}$, 7.8.

nm (haem $b_L$) (c.f. control deconvolutions in legend to Fig. 1). The most dramatic effect of antimycin A was found at pH values where the haem $b_H$ was clearly heterogeneous in control samples, i.e., at high pH. In these cases, antimycin A caused a loss of the high potential form of $b_H$, so that it reverted to a single $n = 1$ species with a midpoint potential close to that of the low potential wave of the control haem $b_H$ (figure 2). In Fig. 4, the midpoint potentials of the best fits to the antimycin A titration data are plotted and can be compared to the $E_m$/pH profiles of the control haem $b_L$ and the low-potential form of haem $b_H$ of figure 3.

*The effects of other inhibitors*

In contrast to antimycin A, myxothiazol caused no detectable change in the heterogeneous redox titration behaviour of haem $b_H$ (Figs. 2 and 5) at any pH value. There was possibly a small increase of the midpoint potential of haem $b_L$, especially at low pH, as if the p$K_{ox}$ of haem $b_L$ had been slightly lowered by myxothiazol. From scrutiny of the detailed spectra, and as already reported [28], the inhibitor caused spectral shifts of both haem groups. The effect on haem $b_H$ was a red shift, whereas the effect on haem $b_L$ was a smaller and opposing blue shift. Individual components could be deconvoluted at 562–568.5 nm (haem $b_H$) and 566–559 nm (haem $b_L$) (c.f. control deconvolutions in legend to Fig. 1).

HQNO and NQNO have been reported to affect both quinone binding sites of the mitochondrial $bc_1$ and chloroplast *bf* complexes [29,30], although with different binding affinities, and they are known to raise the midpoint potential(s) of one [20] or possibly of both [31] haems *b* at pH values close to neutrality. Fig. 5 presents a more detailed picture of the effects of a 5-fold ratio of HQNO/$bc_1$ complex on the redox properties of the haems *b* as a function of pH. The midpoint potential of haem $b_H$ was raised by around 25 mV at all pH values. The effects on haem $b_L$ were less definite. The effects of HQNO at pH 4.8 were studied as a function of HQNO concentration. It was found that its effect on haem $b_H$ was saturated at near stoichiometric amounts of HQNO, consistent with tight binding to the $Q_i$ site with a submicromolar dissociation constant. No large spectral shifts of the *b* haems were found with HQNO.

Stigmatellin has recently been reported to affect the spectra of both haems *b* of the $bc_1$ complex at pH 7.5, and to raise the midpoint potential of haem $b_H$ by 26 mV [32]. Fig. 5 confirms and extends the observation on the midpoint potentials, there being small effects on both $E_m$/pH profiles. By studying difference spectra at appropriate ambient potentials, it was found that the spectrum of haem $b_H$ was shifted to the red, as already known [23], but that the spectrum of haem $b_L$ was relatively unchanged. Individual components could be deconvoluted at 562–570 nm (haem $b_H$) and 566–558.5 nm (haem $b_L$) (c.f. control deconvolutions in legend to Fig. 1). The difference between our results and those of Hauska et al [32], who showed an additional effect of stigmatellin on the spectrum of haem $b_H$, probably arises from the very high concentration of stigmatellin used by these workers. In our experiments with stigmatellin, the haem $b_H$ retained its heterogeneous characteristics at high pH values, a result also consistent with binding only at the $Q_o$ site.

Funiculosin has already been reported to have a dramatic effect on the midpoint potential of haem $b_H$

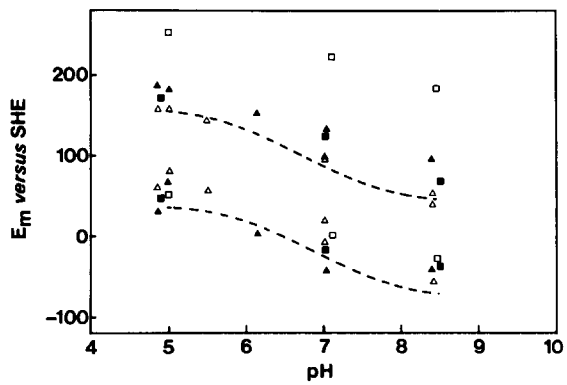


Fig. 5. $E_m$/pH plots of the *b* haems in the presence of myxothiazol. HQNO, stigmatellin or funiculosin. The midpoint potential values of the fits to haem $b_L$ and the low-potential form of haem $b_H$ in the presence of a variety of inhibitors were plotted as a function of pH. The fitted $E_m$/pH curves of the control data from Fig. 3 (dashed lines) have been included for comparison. Inhibitors (all at a 5–10:1 molar ratio in relation to $bc_1$ complex) were: △, myxothiazol; ▲, HQNO; ■, stigmatellin; □, funiculosin. For the myxothiazol data, linear regression best fits for two components, each of which is independently redox-linked to a single protonatable group, gave for haem $b_H$, $E_o$, 155 mV, p$K_{ox}$, 6, p$K_{red}$, 8; and for haem $b_L$, $E_o$, 71 mV, p$K_{ox}$, 5.9, p$K_{red}$, 8.4. For other inhibitors, there were insufficient data points for statistical analyses.

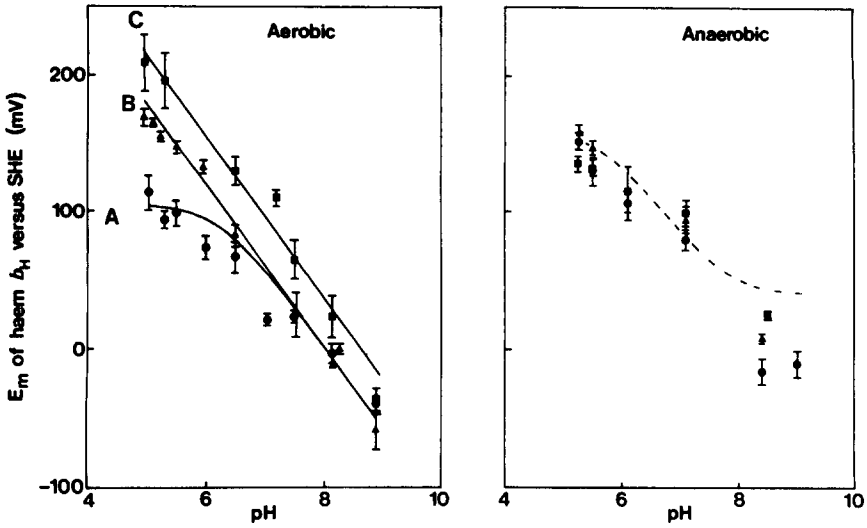


Fig. 6. $E_m$/pH plots of succinate-reducible haem *b* derived from samples poised with the succinate/fumarate redox couple. Titrations of succinate-reducible haem *b* were carried out as described in Materials and Methods, either aerobically in the presence of 1 mM cyanide, or anaerobically under nitrogen and with no inhibitor (●), 10 μM antimycin A (▲), or 10 μM myxothiazol (■). 50% reduction of 'succinate-reducible haem *b*' was taken to be the point at which 25% of the dithionite-reducible signal was developed. Midpoint potentials were calculated by extrapolation of each point on the titration curve to the midpoint with the assumption of an $n = 1$ behaviour. The midpoint potential was calculated from the succinate/fumarate ratio at this point using the succinate/fumarate p$K$ values given by Clark [10] with $E_{m7}$ set to +24 mV. Error bars represent the standard deviations of these estimated midpoint potentials, and are caused mostly by deviations from $n = 1$ behaviour and slight irreversibility of the titrations. In the aerobic titration data, simulated lines are for an $n = 1$ component with a protonatable group of (A) p$K_{ox}$, 6.25; (B) and (C) p$K_{ox}$, < 5. For comparison purposes the behaviour of control haem $b_H$, as determined by conventional redox titration in Fig. 3, is plotted over the anaerobic titration data of the 'succinate-reducible haem *b*' (dotted line in B).

of beef heart mitochondrial $bc_1$ complex at pH 8 [20]. The data in figure 5 confirm and extend this observation by showing that there is an approx. 100 mV increase in the midpoint potential of haem $b_H$ at all pH values. In contrast, the effect on haem $b_L$ was much smaller, with a small but consistent increase in midpoint potential noted at all pH values. For unknown reasons, the haem $b_L$ titration curves were rather poor and heterogeneous and so the significance of its apparent shift in midpoint potential is questionable. The haem $b_H$ titrations corresponded closely to a homogeneous $n = 1$ component at all pH values in the presence of funiculosin. Funiculosin caused the characteristic large blue-shift of haem $b_H$ [23,28], but also had a small effect on the spectrum of haem $b_L$. Individual components could be deconvoluted at 562–570 nm (haem $b_H$) and 566–557 nm (haem $b_L$).

*Characteristics and deconvolution of redox titrations with the succinate/fumarate couple*

Data have already been reported in the literature on the redox titration of the haems *b* with the succinate/fumarate couple [2,12,13,18,19,33]. Some differences in results have been obtained by different groups. In such experiments equilibration occurs via succinate dehydrogenase and endogenous quinone pool. Because of the restricted chemistry which can occur with such biochemical equilibration processes, it is possible that not all redox states of the system are accessible on a reasonable timescale. In such a case the thermodynamic system under study is then not the same and different measured parameters may result. We reinvestigated such redox titrations to see how the results compared with our equilibrium redox titration data.

Several major problems were encountered in attempting quantitative titrations with the succinate/fumarate couple. In the first instance, we were unable to produce complete reversibility of behaviour in the oxidative and reductive directions. Secondly, a maximum of only about 50–60% of the total dithionite-reducible 562 nm peak is reducible by succinate at equilibrium. Since only part of this was haem $b_H$, and since haem $b_H$ contributes 70% of the 562 nm peak (see titration data above), this meant that only about two-thirds of the haem $b_H$ titration curve could be accessed in the titrations. Thirdly, at those pH values where haem $b_H$ had a high potential component, only the low-potential part could be accessed by realisable succinate/fumarate ratios. The above problems made a quantitative analyses difficult. Instead, a somewhat qualitative assessment of midpoint potential was made by treating the succinate-reducible haem *b* (around 50% of the 562 nm peak) as a single component and defining the midpoint potential as that point at which half (defined as 25% of the dithionite-reducible 562 nm peak) became reduced. In practise, the 'succinate-reducible haem *b*' which could be titrated by different succinate/fumarate ratios corresponded very

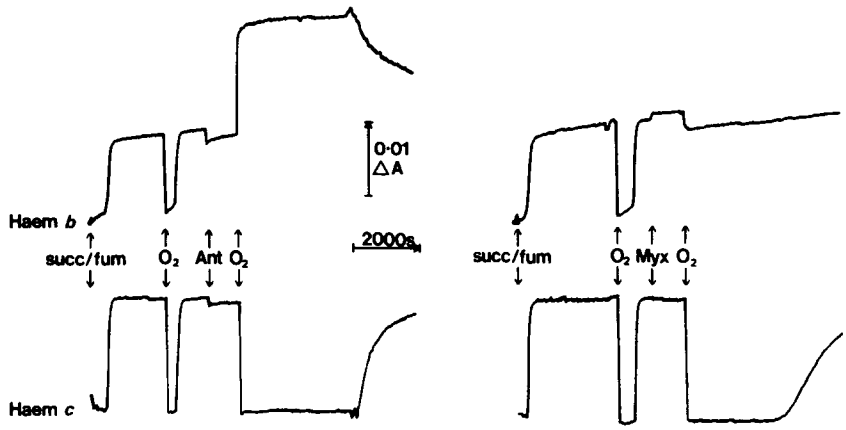


Fig. 7. The effects of myxothiazol and antimycin A on the redox state of haem *b* in succinate/fumarate-poised submitochondrial particles. Beef heart submitochondrial particles were resuspended to around 5 mg/ml in 50 mM Mes, 2 mM EDTA, 1 μM gramicidin and 1 μM valinomycin at pH 5.3 and 20°C. Haems *c* and *b* were monitored at 550–544 nm and 562–580 nm, respectively. Other additions at the points indicated were 10 mM succinate/10 mM fumarate, oxygen (by stirring in air), 10 μM antimycin A or 10 μM myxothiazol.

approximately to the low-potential form of haem $b_H$ which was observed in the titrations of figures 1–5. The high-potential form of haem $b_H$ was not amenable to succinate/fumarate titration and was not considered in our plots.

The first series of experiments were carried out aerobically, but in the presence of cyanide to prevent electron flow through the respiratory chain (Fig. 6A). A pH-dependence of midpoint potential indicative of a component with a $pK_{ox}$ close to 6.5 was found, in agreement with previous reports [13,19]. In addition, when the experiment was repeated in the presence of antimycin A, the data behaved as if this $pK_{ox}$ had been shifted to lower values, again in agreement with previous reports [2,19] and in apparent contrast to the equilibrium data reported above. Further data were collected with myxothiazol present instead of antimycin A. An effect similar to, but less pronounced than, the antimycin A effect was noted. This latter result was particularly surprising since not only was it in contrast to the equilibrium titration data above, but an effect on haem $b_H$ was apparently being caused by an inhibitor of the $Q_o$ site.

Because of these discrepancies, further succinate/fumarate experiments were performed under strictly anaerobic conditions (Fig. 6B). Anaerobiosis was ensured by simultaneous monitoring of the redox state of cytochrome oxidase, data being taken only when the haems *a* were fully reduced. Cyanide was omitted so that the cytochrome oxidase itself removed any last traces of oxygen. In these conditions, quite different $E_m$/pH effects were observed. The redox behaviour of the succinate-reducible haem was roughly the same with or without antimycin A or myxothiazol, being close to the behaviour of the myxothiazol-treated samples in the experiments performed in the presence of cyanide and oxygen. The behaviour of the low-potential form of haem $b_H$, obtained from Fig. 3, has been overlaid on Fig. 6B for comparison. It can be seen that the behaviour of 'succinate-reducible haem *b*' is roughly equivalent.

In order to directly demonstrate qualitatively that the effects of myxothiazol and antimycin A on the midpoint potential(s) of haems *b* are indeed small even at low pH, the experiment of Fig. 7 was performed. The redox poise of haem *b* was clamped in a medium of pH 5.3 with a succinate/fumarate ratio of 1 ($E_{m5.3}$ of succ/fum = +152 mV). This resulted in around 50% reduction of the succinate-reducible haem *b*. Cytochrome ($c + c_1$) were monitored simultaneously as a means of establishing that the sample became fully anaerobic. Antimycin A or myxothiazol were then added directly to this redox poised sample and their effect on the redox state of haems *b* was measured when the sample had become anaerobic again. Provided that the additions were made anaerobically, it was found that antimycin A caused only a very small oxidation, and myxothiazol only a very small reduction, of the haems *b*, consistent with the small effects observed in the equilibrium redox-mediated titrations and inconsistent with the large effects seen in the aerobic, cyanide-inhibited succinate/fumarate titrations of Fig. 6A.

## Discussion

The data on the redox-linked protonations of the haems *b* of the mitochondrial $bc_1$ complex have been incomplete and in some cases equivocal. The present data were obtained in an attempt to provide a more complete picture, since such primary data are essential when interpreting many experiments of current interest which attempt to determine the relative contributions of electrogenic electron transfers and proton transfers to the net protonmotive action of the enzyme.

*Strength of electron/proton coupling of the haems b*

Figs. 2 and 3 clearly show a significant pH-depen-

dence of both haems *b* throughout the pH range 5–9, as is already known. This dependence is, however, significantly less than the −58 mV/pH unit of a strongly coupled system. The simplest model which can fit the data involves two independent protonatable groups, each of whose p$K$ is influenced by the redox state of one haem group. In the case of haem $b_H$, the best fit of this model to the data gives a $pK_{ox}$ and $pK_{red}$ of 5.7 and 7.7, respectively, for its redox-linked protonatable group. In the case of haem $b_L$, the best fit gives values of 5.9 and 7.9. The difference in $pK_{ox}$ and $pK_{red}$ can be taken as a quantitative measure of the strength of proton/electron coupling. For both haems this coupling strength of around 2 pH units may be considered weak (compare, for example, the coupling strength in quinone systems where values above 10 are often encountered).

It should be stressed that the model of a single redox-linked protonatable group associated with each haem *b* is a minimal one and other possibilities exist. For example, Maróti and Wraight [34,35] and McPherson et al. [36] have shown with the bacterial reaction centre that redox linked protonation changes may involve several different protonatable groups with overlapping p$K$ values, even when the $E_m$/pH dependence is −60 mV/pH unit or less. The data in Fig. 3 could also be simulated with a model involving a large number of protonatable groups which are very weakly coupled to one or other haem redox state. The data cannot, however, be simulated with a model involving a single protonatable group whose p$K$ is affected by the redox state of both haems *b* (we have recently invoked such a model for the pH-dependence of midpoint potentials of haem *a* and $Cu_B$ of cytochrome oxidase [37]).

*Redox interaction between the haems b?*

An unresolved point concerns possible redox interaction between the two haems *b*. Because of the predicted locations of the haems [38–40], and by analogy with the redox centres in cytochrome oxidase [41], such redox interaction might be expected. However, the measurable potentials of haem $b_H$ (with $b_L$ oxidised) and of haem $b_L$ (with $b_H$ reduced) are separated by around 100 mV over the accessible pH range. Unless there were a redox interaction of this about this size, we would be unable to detect the effects of such interaction on the shape of the redox curve of each component. We are therefore able only to say that any such redox interaction between the haems must be less than 100 mV. It would be of interest to know the value more accurately, since it would allow us to know the true equilibrium constant, and therefore the energy available, in the electrogenic reaction:

$$b_L^- b_H \rightarrow b_L b_H^-$$

*Effects of inhibitors on midpoint potentials and redox-linked protonations*

Effects of a variety of inhibitors on the midpoint potentials [20,42] and optical spectra [28] of the haems *b* have already been reported. Our results generally confirm and extend these findings. Most inhibitors have a rather small effect on the haem *b* potentials and spectra. In those cases where effects can be measured, the haem which is closest to the site of inhibitor binding is generally the most affected. Hence, the o-site inhibitor myxothiazol affected spectroscopically and potentiometrically mostly haem $b_L$ whereas the i site inhibitors antimycin A and funiculosin affect spectroscopically and potentiometrically mostly haem $b_H$. Although HQNO probably binds to both sites at high concentrations, we noted a definite effect only on the midpoint potentials of haem $b_H$. Of all inhibitors tested, only funiculosin caused a particularly dramatic shift (around 100 mV) in midpoint potentials (of haem $b_H$). We were unable to detect any large effect of stigmatellin on the spectral properties of haem $b_H$, in contrast to Ref. 32, and this difference may be due to the very much lower inhibitor concentrations used in our studies, although we were able to detect a small effect on the midpoint potentials of both haems *b*. The most notable anomaly was the effect of myxothiazol on the spectrum of haem $b_H$. This has been noted previously with beef heart submitochondrial particles [28], but is in contrast to results with isolated enzyme [43]. However, it is likely that these small spectral changes can be quite different in isolated, compared to membranous, enzyme because of detergent effects on the haem *b* spectra (for example, compare Refs. 44 and 45) and they also appear to vary with mitochondria from different sources ( see for example, Ref. 42). Some secondary effects of binding of inhibitors which affect the most distant haem *b* are perhaps not surprising since some global perturbation of the α-helical bundles might be expected on binding of these hydrophobic molecules.

In no instance was the pH-dependence of midpoint potentials of the haems *b* altered dramatically by inhibitor binding. This suggests that none of the inhibitors binds directly to the redox-linked protonatable groups.

*Interpretation and modelling of the heterogeneous redox behaviour of haem $b_H$ at high pH*

As illustrated in Fig. 2, the redox titration curve of haem $b_H$ became heterogeneous at pH values of 7 and above, with a new high potential wave becoming progressively more prominent. A high-potential wave has been observed previously [18] and it has been suggested that the two waves represent two functionally different forms of $b_H$ which are predicted in the dimeric mechanistic model [22]. More recently, Salerno [21] observed two forms of haem $b_H$ at pH 7.2–7.4 with different

EPR and potentiometric characteristics and suggested that this might arise from the occupation of the $Q_i$ site by different redox forms of ubiquinone. Our data show that the heterogeneous behaviour is removed by i-site inhibitors, but not by o-site inhibitors. Since this is consistent with the model proposed by Salerno, we sought to simulate a relatively simple version in order to determine whether the behaviour was consistent with the known potentiometric behaviour of bound quinone. The model assumes that haem $b_H$ and bound quinone interact so that the midpoint potential of one species is dependent on the redox state of the other. The simplest form is shown schematically in Fig. 8 (top) and involves seven microscopic midpoint potentials. The data points in Fig. 8 are redox titrations of haem $b_H$ alone, deconvoluted at 562–569 nm from the data at pH 7.05 and 8.45 of Fig. 2. The computer was also provided with the known redox behaviour of EPR-detectable ubisemiquinone, taken from Refs. 46–48. This ubisemiquinone was assigned at pH 7.05 with $E_m = 81$ mV, EPR-detectable semiquinone *per* $bc_1$ at peak = 0.1; half peak width = 73 mV and at pH 8.45 with $E_m = 0$ mV, EPR-detectable semiquinone *per* $bc_1$ at peak = 0.5; half peak width = 91 mV. One unconventional feature of the model was that only semiquinone (protonated and unprotonated forms) bound to reduced haem $b_H$ was assumed to be EPR-detectable. The solid lines in Fig. 8 represent the linear least-squares best fit of this model to the haem $b_H$ and the observed semiquinone data. It is clear that such a simple model can, in principle, reproduce observed behaviour quite closely whilst using values of potentials and stability constants of the bound quinone which reproduce experimentally observed semiquinone behaviour [46–49]. In addition, as the pH is lowered below 7 the quinone system retains a −58 mV/pH unit pH-dependence [47,48] whereas the haem $b_H$ becomes only weakly pH-dependent. As a result, by pH 4.8 the quinone system becomes fully reduced before the haem $b_H$ system begins to titrate so that the model predicts only a single $n = 1$ component of haem $b_H$ at pH 4.8, as was observed experimentally (Fig. 1).

These simulations were based on the assumption that only semiquinone which is bound to a reduced haem $b_H$ is EPR-detectable. There is some experimental justification for this, since it has been shown with the yeast enzyme that oxidised haem $b_H$ and semiquinone are spin-coupled and EPR silent [50,51]. In fact, we were unable to successfully simulate data if we assumed that all forms of semiquinone are EPR-detectable. This failure arises because the bound quinone system titrates at too low a potential to produce the observed haem $b_H$ distortions when it is assumed that all semiquinone is EPR-detectable. The possibility of significant amounts of EPR-silent semiquinone has not been taken into account in previous analyses of the microscopic potentials of the bound semiquinone system [46–49]. Our

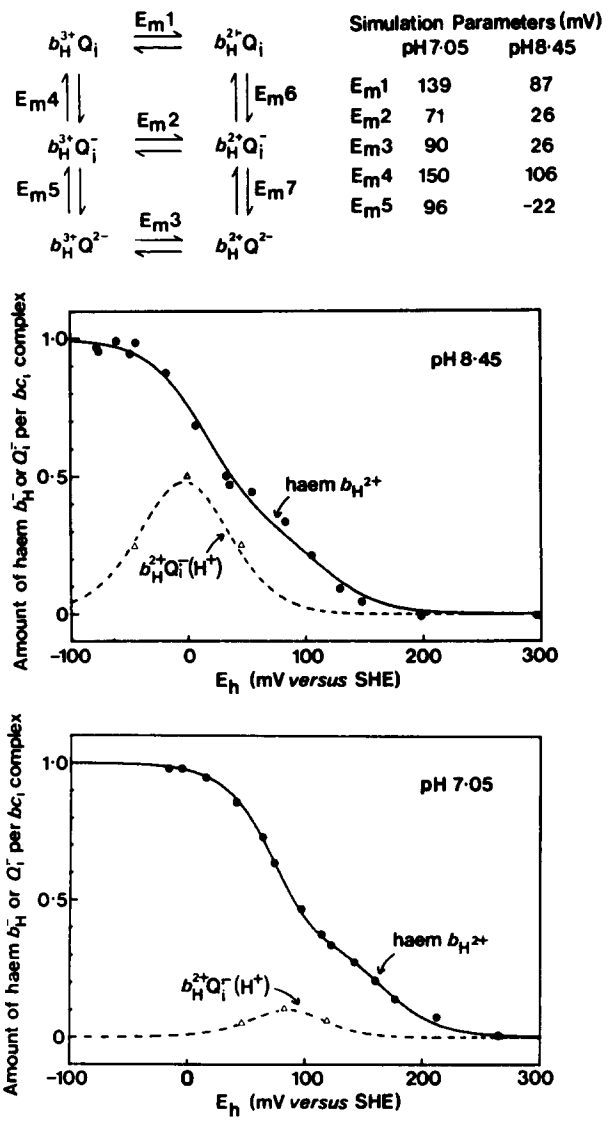


Fig. 8. Simulated behaviour of the redox titration curves of haem $b_H$ and EPR-detectable semiquinone. Haem $b_H$ titration behaviour (●) at pH 7.05 or 8.45 was deconvoluted from the control data of Fig. 2 at 562–569 nm. Estimated behaviour of EPR-detectable semiquinone (△) was taken from [46–48] as described in the text. All semiquinone species bound to oxidised haem $b_H$ were assumed to be EPR-silent. The least squares best fit values of midpoint potentials $E_{m1}$ to $E_{m5}$ to the haem $b_H$ data and to three data points (peak and half peak coordinates) of EPR-detectable semiquinone are tabulated above. $E_{m6}$ and $E_{m7}$ are automatically fixed by these five values. The simulated behaviour of haem $b_H$ (solid line) and semiquinone species bound to haem $b_H^{2+}$ (dashed line) using these best fit values are plotted over the data. For clarity in the illustration of the model used for simulation (top), the dominant degree of protonation of each quinone species has not been drawn.

simulations have shown that such EPR-silent semiquinone could contribute significantly to the total semiquinone profile. Fig. 9 again shows the simulation of EPR-observable semiquinone at pH 7.05, taken from Fig. 8, and compares it to the total semiquinone which the model predicts to be present. It is clear that, if one form of semiquinone is indeed EPR silent, the previ-

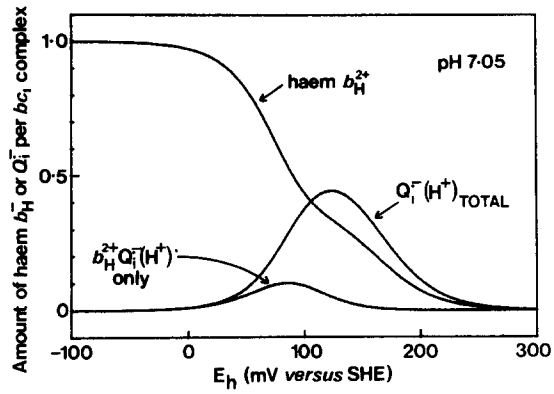


Fig. 9. A comparison of simulated redox titration behaviour of EPR-detectable and total i-site semiquinone. The best fit pH 7.05 simulation data of Fig. 8 are replotted together with the predicted titration behaviour of total (i.e., EPR-detectable *plus* EPR-silent) semiquinone species.

ously-estimated microscopic constants of the bound $Q_i$ system may have to be significantly reassessed. It may also form the basis of an explanation for the lack of detection of significant semiquinone in the analogous chloroplast cytochrome *bf* complex. In the *bf* system, the midpoint potentials of the haems *b* are much lower and most semiquinone will be present when haem $b_H$ is oxidised. These possibilities require further investigation.

It should be noted that the model of Fig. 8 represents only one simple version and other factors, such as binding constants of different Q species [47], have not been included, since the data quality does not warrant such complexity. Nevertheless the simulations indicate that this type of model can in principle reproduce observed experimental features, makes new testable predictions, and in our opinion is the most reasonable explanation to date of the multiple redox forms of haem $b_H$.

*Succinate/fumarate titrations and their relation to equilibrium redox-mediated data*

It is now clear that redox titration with the succinate/fumarate couple of 'succinate-reducible haem *b*' is not amenable to precise analysis, since the titratable component is composed of a major part of sometimes heterogeneous haem $b_H$, together with a small fraction of haem $b_L$. Early reports of such titrations did not necessarily take such complications into account and so may differ somewhat from our own analyses. Nevertheless, since the accessible titration range with succinate/fumarate is close to that of the low potential form of haem $b_H$, there is some correspondance between the values which we obtain for the low-potential form of haem $b_H$ and the redox behaviour of 'succinate-reducible haem *b*' under strictly anaerobic conditions (compare Figs. 6B and 3). The high-potential form of haem $b_H$ which is observed at high pH in dye-mediated titrations is not easily accessible with succinate/fumarate and was not taken into account in our analyses. The succinate/fumarate data exhibit an average pH dependence of about −40 mV/pH unit between pH 5 and 8 and neither antimycin A nor myxothiazol causes large changes in estimated midpoint potential. The data in Fig. 7 confirm in a very direct way this extremely small degree of antimycin- or myxothiazol-induced changes of midpoint potential of haems *b* at pH 5.3.

Previously, it has been thought that succinate/fumarate titration data were consistent with a $pK_{ox}$ of around 6.5 for $b_H$ [13] and that antimycin A lowered the $pK_{ox}$ so that the haem *b* retained a −58 mV/pH dependence down to at least pH 5 [2,19]. Such effects could be repeated in our hands only when the titrations were performed aerobically in the presence of cyanide (Fig. 6A). The anaerobic titrations (Fig. 6B) corresponded most closely to the aerobic titrations which were performed with myxothiazol present. It is suggested that, under aerobic conditions with cyanide present, the control and antimycin A titration data do not indicate the true equilibrium thermodynamic $E_m$/pH behaviour of haem *b*, especially at low pH, because of slow leaks through the system. In the case of the aerobic titration with antimycin A present, a slow leak through cytochrome oxidase at low pH may cause additional oxidant-induced reduction of haem *b* and so raise its apparent midpoint potential. In the case of the control aerobic titration, this slow leak, together with a significant inhibition of succinate dehydrogenase at low pH, may prevent the quinone pool attaining as low an $E_h$ as the added succinate/fumarate couple, thereby lowering the apparent midpoint potential of the 'succinate-reducible haem *b*'.

*Implications in relation to possible electrogenic proton transfers through the enzyme*

The present work shows that each haem *b* has one weakly coupled, or possibly many very weakly coupled, redox-linked protons. The binding of o-site or i-site inhibitors appears not to affect this coupling significantly. Since these inhibitors are always rather hydrophobic molecules which bind into hydrophobic sites, this suggests that the protonation changes might occur on residues in a hydrophilic phase, rather than on critical residues buried in the hydrophobic domain of the $Q_o$ or $Q_i$ sites.

On the basis of the effects of sided pH pulses on vesicle-incorporated, redox-clamped $bc_1$ complex, Konstantinov and Popova suggested [7] that protonation of haem $b_H$ in the presence of antimycin A occurred from the centre o-side of the complex. Since, however, it is clear that haem $b_H$ does not have a pH-dependence of midpoint potential of −58 mV/pH even with antimycin A present (this work), it is most likely that their observations of a lack of $pH_i$ effect on

antimycin-inhibited, $Q/QH_2$-poised enzyme [7] is caused by inhibition of redox equilibration mechanisms, rather than by a $Q_o$-sided haem $b_H$-linked protonation process.

It is also now well documented that inhibition of reoxidation of haem $b_H$ is accompanied by a loss of around half of a charge transfer across the membrane [4,52]. Inhibition has been best achieved with antimycin A or H(N)QNO. Since, however, the above data show that the associated protonation changes of haem $b_H$ are unaffected by these inhibitors, it can be reasonably be concluded that loss of electrogenicity is caused by inhibition of electron transfer to $Q_i$ and is not associated with the prevention of an electrogenic protonation of haem $b_H$.

It would appear likely from the above arguments that the major electrogenic reactions of the catalytic cycle of the cytochrome $bc_1$ complex are electron transfers, and that associated (de)protonations which result in a net proton translocation are themselves electroneutral. This means that the protons do not travel along proton *wells* [8,53] of low dielectric strength. However, it is still feasible that they could move considerable distances through the protein structure along proton *channels* in a non-electrogenic manner, provided that these channels are of high dielectric strength or provided that they allow the synchronous movement of counterions [24].

## Acknowledgements

This work is supported by the United Kingdom SERC (grant no. GR/E53941) and by the benefactors of the Glynn Research Foundation Ltd. Submitochondrial particles were prepared, and figures produced, by Mr. R. Harper. Stigmatellin was a generous gift of Professor Dr. G. Höfle. We benefited greatly from discussions of the work with Dr. P. Mitchell.

## References

1 Mitchell, P. (1976) J. Theor. Biol. 62, 327–367.
2 Gopher, A. and Gutman, M. (1980) J. Bioenerg. Biomemb. 12, 349–367.
3 Jones, R.W. and Whitmarsh, J. (1985) Photobiochem. Photobiophys. 9, 119–127.
4 Robertson, D.E. and Dutton, P.L. (1988) Biochim. Biophys. Acta 935, 273–291.
5 West, I.C., Mitchell, P. and Rich, P.R. (1988) Biochim. Biophys. Acta 933, 35–41.
6 Hope, A.B. and Rich, P.R. (1989) Biochim. Biophys. Acta 975, 96–103.
7 Konstantinov, A.A. and Popova, E. (1987) in Cytochromes: Molecular Biology and Bioenergetics (Papa, S., Chance, B. and Ernster, L., eds.), pp. 751–765, Plenum, New York.
8 Mitchell, P. (1968) Chemiosmotic Coupling and Energy Transduction, Glynn Research, Bodmin.
9 Rich, P.R., Moody, A.J. and Mitchell, R. (1989) in Charge and Field Effects in Biosystems (Allen, M.J., ed.), pp. 9–21, Plenum, New York.
10 Clark, W.M. (1960) Oxidation-Reduction Potentials of Organic Systems, Bailliere, Tindall and Cox, London.
11 Dutton, P.L. and Wilson, D.F. (1974) Biochim. Biophys. Acta 346, 165–212.
12 Straub, J.P. and Colpa-Boonstra, J.P. (1962) Biochim. Biophys. Acta 60, 650-652.
13 Urban, P.F. and Klingenberg, M. (1969) Eur. J. Biochem. 9, 519–525.
14 Wilson, D.F., Erecinska, M., Leigh, J.S., Jr. and Koppelman, M. (1972) Arch. Biochem. Biophys. 151, 112–121.
15 Dutton, P.L., Erecinska, M., Sato, N., Mukai, Y., Pring, M. and Wilson, D.F. (1972) Biochim. Biophys. Acta 267, 15–24.
16 Nelson, B.D. and Gellerfors, P. (1974) Biochim. Biophys. Acta 357, 358–364.
17 Riccio, P., Schägger, H., Engel, W.D. and Von Jagow, G. (1977) Biochim. Biophys. Acta 459, 250–262.
18 Berden, J.A. and Opperdoes, F.R. (1972) Biochim. Biophys. Acta 267, 7–14.
19 Kamenskii, Y.A., Artzatbanov, V.Y., Shevchenko, D.V. and Konstantinov, A.A. (1979) Dokl. Acad. Nauk. (USSR) 249, 994–997.
20 Kunz, W.S. and Konstantinov, A.A. (1983) FEBS Lett. 155, 237–240.
21 Salerno, J.C., Xu, Y., Osgood, M.P., Kim, C.H. and King, T.E. (1989) J. Biol. Chem. 264, 15398–15403.
22 De Vries, S., Albracht, S.P.J., Berden, J.A. and Slater, E.C. (1982) Biochim. Biophys. Acta 681, 41–53.
23 Von Jagow, G. and Link, T.A. (1986) Methods Enzymol. 126, 253–271.
24 Rich, P.R. (1990) in Structure, Function and Biogenesis of Energy Transfer Systems (Papa, S., ed.), Elsevier, in press.
25 Smith, A.L. (1967) Methods Enzymol. 10, 81–86.
26 White, J.H., Soriaga, M.P. and Hubbard, A.T. (1985) J. Electroanal. Chem. 185, 331–338.
27 Yu, L., Xu, J-X., Haley, P.E. and Yu, C-A. (1987) J. Biol. Chem. 262, 1137–1143.
28 Kamensky, Y., Konstantinov, A.A., Kunz, W.S. and Surkov, S. (1985) FEBS Lett. 181, 95–99.
29 Papa, S., Izzo, G. and Guerrieri, F. (1982) FEBS Lett. 145, 93–98.
30 Riccio, P., Bobba, A. and Quagliariello, E. (1982) FEBS Lett. 137, 222–226.
31 Clark, R.D. and Hind, G. (1983) Proc. Natl. Acad. Sci. USA 80, 6249–6253.
32 Hauska, G., Herold, E., Huber, C., Nitschke, W. and Sofrova, D. (1989) Z. Naturforsch. 44c, 462–467.
33 Wikström, M.K.F. and Berden, J.A. (1972) Biochim. Biophys. Acta 283, 403–420.
34 Maróti, P. and Wraight, C.A. (1988) Biochim. Biophys. Acta 934, 314–328.
35 Maróti, P. and Wraight, C.A. (1988) Biochim. Biophys. Acta 934, 329–347.
36 McPherson, P.H., Okamura, M.Y. and Feher, G. (1988) Biochim. Biophys. Acta 934, 348–368.
37 Moody, A.J. and Rich, P.R. (1990) Biochim. Biophys. Acta, 1015, 205–215.
38 Saraste, M. (1984) FEBS Lett. 166, 367–372.
39 Widger, W.R., Cramer, W.A., Herrmann, R.G. and Trebst, A. (1984) Proc. Natl. Acad. Sci. USA 81, 674–678.
40 Ohnishi, T., Schägger, H., Meinhardt, S.W., LoBrutto, R., Link, T.A. and Von Jagow, G. (1989) J. Biol. Chem. 264, 735–744.
41 Wikström, M., Krab, K. and Saraste, M. (1981) Cytochrome Oxidase. A Synthesis, Academic Press, London.
42 Tsai, A-L., Kauten, R. and Palmer, G. (1985) Biochim. Biophys. Acta 806, 418-426.
43 Becker, W.F., Von Jagow, G., Anke, T. and Steglich, W. (1981) FEBS Lett. 132, 329–333.
44 Von Jagow, G. and Engel, W.D. (1981) FEBS Lett. 136, 19–24.

45 Thierbach, G. and Reichenbach, H. (1981) Biochim. Biophys. Acta 638, 282–289.
46 Robertson, D.E., Prince, R.C., Bowyer, J.R., Matsuura, K., Dutton, P.L. and Ohnishi, T. (1984) J. Biol. Chem. 259, 1758–1763.
47 De Vries, S., Berden, J.A. and Slater, E.C. (1980) FEBS Lett. 122, 143–148.
48 Ohnishi, T. and Trumpower, B.L. (1980) J. Biol. Chem. 255, 3278–3284.
49 De Vries, S. (1983) Ph.D. Thesis. University of Amsterdam.
50 Siedow, J.N., Power, S., De la Rosa, F.F. and Palmer, G. (1978) J. Biol. Chem. 253, 2392–2399.
51 De la Rosa, F.F. and Palmer, G. (1983) FEBS Lett. 163, 140–143.
52 Jones, R.W. and Whitmarsh, J. (1988) Biochim. Biophys. Acta 933, 258–268.
53 Mitchell, P. (1977) in Symposia of the Society of General Microbiology XXVII. Microbial Energetics, pp. 383–423.